

Lower Pseudogap Phase: A Spin/Vortex Liquid State

Zheng-Yu Weng and Xiao-Liang Qi

Center for Advanced Study, Tsinghua University, Beijing 100084, China

The pseudogap phase is considered as a new state of matter in the phase string model of the doped Mott insulator, which is composed of two distinct regimes known as the *upper* and *lower* pseudogap phases, respectively. The former corresponds to the formation of spin singlet pairing whose magnetic characterizations have been recently studied [Phys. Rev. B **72**, 104520 (2005)]. The latter as a low-temperature regime of the pseudogap phase is systematically explored in this work, which is characterized by the formation of the Cooper pair amplitude and described by a generalized Ginzburg-Landau theory. Elementary excitation in this phase is a charge-neutral object carrying spin-1/2 and locking with a supercurrent vortex, known as spinon-vortex composite. Such a lower pseudogap phase can be regarded as a vortex liquid state due to the presence of free spinon-vortices. Here thermally excited spinon-vortices destroy the phase coherence and are responsible for nontrivial Nernst effect and diamagnetism. The transport entropy and core energy associated with a spinon-vortex are determined by the spin degrees of freedom. Such a spontaneous vortex liquid phase can be also considered as a spin liquid with a finite correlation length and gapped $S = 1/2$ excitations, where a resonancelike non-propagating spin mode emerges at the antiferromagnetic wavevector (π, π) with a doping-dependent characteristic energy. The superconducting phase is closely related to the lower pseudogap phase by a topological transition with spinon-vortices and -antivortices forming bound pairs and the emergence of fermionic quasiparticles as holon-spinon-vortex bound objects. A quantitative phase diagram in the parameter space of doping, temperature, and magnetic field is determined. Comparisons with experiments are also made.

I. INTRODUCTION

Pseudogap phenomenon^{1,2} in the underdoped cuprates is widely considered to be closely related to the high- T_c problem. Any sensible microscopic theory for the high- T_c superconductivity is expected to include the pseudogap as an integral part of the theory concerning the high-temperature/energy and short-distance physics. Due to the unconventional properties manifested^{1,2} in transport, spin dynamics, optical and single-particle spectroscopies, thermodynamic properties, etc., experimental measurements in the pseudogap regime have imposed much *stronger* constraints on a potential high- T_c theory than just those in the superconducting state.

Experimentally two distinctive pseudogap regions have been observed^{1,3,4,5,6}. The high-temperature (T) regime, called the *upper* pseudogap phase (UPP), is marked by the suppression of uniform magnetic susceptibility^{7,8} and the deviation of dc resistivity from the linear-T behavior^{8,9,10}, both of which happen below a characteristic temperature T_0 . The temperature T_0 is comparable to the superexchange coupling strength ($\sim 1,000$ K) near the half-filling and decreases monotonically with doping^{7,8,9,10}. Near the optimal doping, T_0 is reduced to the same order of magnitude as the superconducting transition temperature T_c . The single-particle pseudogap structure around the wavevector $(\pm\pi, 0)$ and $(0, \pm\pi)$ observed in the ARPES experiments¹¹ also shows a similar doping dependence. A low-T pseudogap regime, called the *lower* pseudogap phase (LPP), corresponds to a crossover regime between the UPP and superconducting (SC) phase, where the low-energy antiferromagnetic (AF) fluctuations get suppressed as shown in ⁶³Cu NMR experiments^{3,12}, accompanied by the emergence of a “high-energy” (“41 meV”) resonancelike peak in the dynamic spin susceptibility function around the AF wavevector (π, π) as revealed by the neutron measurements¹³.

One of the most significant experimental observations in the LPP region is the discovery^{14,15,16,17,18,19,20} of the large Nernst signal and residual diamagnetism which strongly support the presence of vortex excitations²¹ in a wide temperature range which can be several times higher than T_c at low doping. Generally it is believed that the superconducting phase transition in underdoped materials is due to the phase disordering effect²² by vortices as one approaches T_c from below. There have been a number of theoretical proposals^{22,23,24,25,26,27} to explain the existence of topological vortices above T_c in the underdoped regime. However, the nature of these vortices above T_c can vary distinctly from the more conventional Kosterlitz-Thouless (KT) vortices^{22,25,26} to exotic vortices with a spin-1/2 (spinon) trapped at each core²³.

It would be rather difficult for one to judge the relevance of a particular microscopic theory simply in terms of some detailed account for individual experiments, considering huge amounts of existing data available for interpretation and the lack of consensus on the underlying mechanism after almost two decades’ extensive and intensive investigations. It is thus particularly meaningful for a potential microscopic theory of high- T_c to be worked out extensively and self-consistently to provide a comprehensive “road map”. One may then use the obtained specific “map” and organizing principles to accommodate and analyze the experimental results with priority and hierarchy, and to further predict new experiments. Only in this way may one effectively justify or falsify a particular theoretical approach based on a

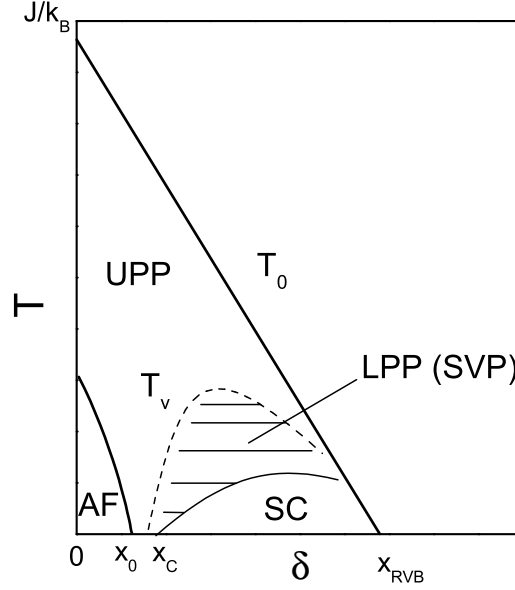


FIG. 1: The global phase diagram of the phase string model at low doping²⁸. The high-temperature phase is called the upper pseudogap phase (UPP) which is characterized by the bosonic RVB order parameter Δ^s and the temperature T_0 . The antiferromagnetic (AF) long-range order state, the lower pseudogap phase (LPP) which is also called²³ the spontaneous vortex phase (SVP) with a characteristic temperature T_v , and the d-wave superconducting phase (SC) below T_c , all occur as some forms of low-T instabilities in the UPP. For example, the AF state corresponds to the spinon condensation on the RVB background, while the LPP and SC states involve the holon condensation. The detailed phase diagram is determined by the unique mutual duality gauge structure^{31,32} which quantitatively governs the intrinsic competition between the charge and spin degrees of freedom. The shaded regime of the LPP will be the main focus of this work.

broad set of experimental measurements.

The “road map” of the phase string model²⁸ is illustrated by a global phase diagram at low doping in Fig. 1. This model is an effective theory proposed for the cuprate superconductors based on the $t - J$ model, with a careful treatment of the spin correlation at various ranges and with *self-consistently* incorporating the mutual interplay between the spin and charge degrees of freedom^{28,29,30,31,32,33}. Such a model describes a doped Mott insulator with spins forming singlet pairing, known as the bosonic resonating-valence-bond (RVB) pairing, in the UPP. The magnetic characterizations of this phase have been carefully examined in Ref.³⁴ recently. At half-filling, without the presence of holes, the short-range AF correlations in the UPP will *continuously* grow with reducing temperature and eventually becomes AF long-range ordered (AFLRO) in the ground state (a finite Néel temperature will be the consequence of the interlayer coupling). On the other hand, as doped holes moving in the spin background always generates the so-called phase string effect²⁹, the spin dynamics³⁵ will be drastically reshaped beyond some doping concentration³¹, in order for holes to further gain kinetic energy³⁶ at low-T. In such a finite doping regime, one enters the LPP [also known as the spontaneous vortex phase (SVP)²³] at a low temperature T_v and finally ends up in the SC state^{37,38} below T_c without encountering an AFLRO.

The above global phase diagram with the UPP as the high-T “unstable fixed point” state of the doped Mott insulator is spiritually very similar to the proposals made by Anderson^{27,39} recently, where the LPP and SC phases are considered as low-energy/temperature instabilities with the spin-charge “locking” evolving progressively. Although two approaches look different mathematically, they still share some important features like the RVB spin pairing in the UPP, vortex liquid state in the LPP, and vortex-antivortex binding in the SC, as well as the kinetic-energy-driven and progressive charge-spin recombination in the latter regimes. The main distinction between the two approaches perhaps lies in how the UPP is described as the high-energy/temperature starting point. In a framework based on the Gutzwiller-projected *fermionic* RVB (f-RVB) mean-field state^{2,40}, the short-range AF correlations are normally intrinsically weak, *before the Gutzwiller projection*, as compared to those in the *bosonic* RVB state, such that the

kinetic energy of doped holes at the mean-field level is not as severely frustrated. The advantage of this approach is that the coherent fermion nodal quasiparticle appears directly in the formalism. By contrast, in the bosonic RVB state, the short-range AF correlations are intrinsically associated with the bosonic RVB pairing, which remain strong even *before* the Gutzwiller projection is made or in other words, at the mean-field level, such that the motion of doped holes always gets severely frustrated in the UPP. Consequently, with decreasing temperature, the tendency for gaining the kinetic energy becomes the critical driving force to realize the LPP and SC at a finite doping. Here the fermion nodal quasiparticle emerges as a coherent one only in the SC state through a more delicate spin-charge binding process⁴¹. It is also noted that the gauge structure describing the fluctuations around the mean-field state, which is either $U(1)$ ^{42,43}, $SU(2)$ ⁴⁴ or even Z_2 ⁴⁵, arising from the no double occupancy constraint in the slave-boson approaches^{2,40} based on the f-RVB description, is rather different from the present mutual duality (mutual Chern-Simons³²) gauge structure arising from the phase string effect in the $t - J$ model²⁹. The latter is crucially responsible for the global phase diagram shown in Fig. 1, occurring at proper temperatures and doping regions as compared to the experiments.

In this paper, we will present a systematic and detailed description of the LPP (the shaded region in Fig. 1) based on the phase string model in the context of the global phase diagram involving the UPP, SC, and AF phases. The basic picture is that the pseudogap phase is a new state of matter, which is a doped Mott insulator with spin-charge separation. In particular, the LPP is characterized by the holon condensation, described by a generalized Ginzburg-Landau (GL) theory^{23,37}. The elementary excitation identified in this phase is a bosonic charge-neutral object carrying spin-1/2 and vortexlike currents known as a spinon-vortex. The LPP is composed of thermally excited spinon-vortices which destroy the SC phase coherence, while the Cooper pair amplitude still remains. Interesting consequences of this phase will be explored, including the Nernst effect and diamagnetism. How the LPP is closely related to the SC phase by a topological transition involving vortex-antivortex binding or “spinon confinement”, including the emergence of coherent *fermionic* quasiparticles in the SC phase⁴¹, will be also discussed.

The remainder of the paper is organized as follows. In Sec. II, the theoretical framework of the phase string model is presented and the elementary equations describing the LPP are given. In Sec. III, the physical properties of the LPP are explored, including the spin liquid behavior, elementary excitation, phase diagram, the Nernst effect and diamagnetism, as well as the topological transition to the SC state. Finally, a summary and conclusions are presented in Sec. IV.

II. ELEMENTARY EQUATIONS

A. Phase string model

The phase string model is an effective low-energy theory, obtained^{30,33} based on the phase string formulation of the two-dimensional (2D) $t - J$ model, in which the electron annihilation operator is decomposed in the following *bosonization* form²⁹

$$c_{i\sigma} = h_i^\dagger b_{i\sigma} e^{i\Theta_{i\sigma}} \quad (1)$$

where both holon h_i^\dagger and spinon $b_{i\sigma}$ operators are bosonic fields, satisfying the no-double-occupancy constraint $n_i^h + \sum_\sigma n_{i\sigma}^b = 1$ with $n_i^h = h_i^\dagger h_i$ as the holon number and $n_{i\alpha}^b = b_{i\alpha}^\dagger b_{i\alpha}$ as the spinon number. The phase factor $e^{i\Theta_{i\sigma}}$, which ensures the fermionic statistics of $c_{i\sigma}$, is defined by $e^{i\Theta_{i\sigma}} \equiv e^{i\Theta_{i\sigma}^{string}} (\sigma)^{\hat{N}_h} (-\sigma)^i$, where \hat{N}_h is the total holon number operator, $\sigma = \pm 1$, and $(-1)^i = \pm 1$ ($i \in$ even/odd site) is a staggered sign factor. The phase $\Theta_{i\sigma}^{string} \equiv \frac{1}{2} [\Phi_i^s - \Phi_i^0 - \sigma \Phi_i^h]$ is a nonlocal operator with

$$\Phi_i^s = \sum_{l(\neq i)} \text{Im} \ln (z_i - z_l) \left(\sum_\alpha \alpha n_{l\alpha}^b \right), \quad (2)$$

$$\Phi_i^0 = \sum_{l(\neq i)} \text{Im} \ln (z_i - z_l), \text{ and}$$

$$\Phi_i^h = \sum_{l(\neq i)} \text{Im} \ln (z_i - z_l) n_l^h, \quad (3)$$

where $z_l = x_l + iy_l$ is the complex coordinate for a lattice site l .

The effective phase string theory is a *bosonic* RVB theory, in which the spin degrees of freedom are described by the following spinon Hamiltonian:

$$H_s = -J_s \sum_{\langle ij \rangle \sigma} \left[\left(e^{i\sigma A_{ij}^h} \right) b_{i\sigma}^\dagger b_{j-\sigma}^\dagger + \text{H.c.} \right] - \lambda \sum_{i\sigma} \left(b_{i\sigma}^\dagger b_{i\sigma} - \frac{1-\delta}{2} \right) . \quad (4)$$

Here the effective coupling constant $J_s = J(1-g)\Delta^s/2$, where J is the superexchange constant in the original $t-J$ model, $g \simeq 4\delta$ with δ denoting the doping concentration stands for a renormalization effect to the superexchange energy J ,³⁴ and Δ^s is the bosonic RVB order parameter defined by

$$\Delta^s = \sum_{\sigma} \left\langle e^{-i\sigma A_{ij}^h} b_{i\sigma} b_{j-\sigma} \right\rangle_{\text{NN}} \quad (5)$$

with the sites i and j belonging to two nearest neighbors (NN). The Lagrangian multiplier λ enforces the constraint $\sum_{\sigma} \langle b_{i\sigma}^\dagger b_{i\sigma} \rangle = 1 - \delta$.

The charge degree of freedom is governed by the holon Hamiltonian

$$H_h = -t_h \sum_{\langle ij \rangle} \left(e^{iA_{ij}^s + ieA_{ij}^e} \right) h_i^\dagger h_j + \text{H.c.} \quad (6)$$

where $t_h \sim t$ (t is the hopping integral in the original $t-J$ model) is the renormalized hopping integral for holons, which directly see the external electromagnetic vector potential A_{ij}^e with charge $+e$.

A peculiar feature of the phase string model is that the spinons and holons see two *different* gauge fields, A_{ij}^h and A_{ij}^s , with their strengths constrained to the densities of *holons* and *spinons*, respectively. Namely, A_{ij}^h and A_{ij}^s satisfy the following gauge-independent topological constraint

$$\oint_c d\mathbf{r} \cdot \mathbf{A}^h = \pi N^h(c) \quad (7)$$

$$\oint_c d\mathbf{r} \cdot \mathbf{A}^s = \pi [N_{\uparrow}^b(c) - N_{\downarrow}^b(c)] \quad (8)$$

where \mathbf{A}^h and \mathbf{A}^s are defined by $A_{ij}^h \equiv \mathbf{r}_{ij} \cdot \mathbf{A}^h$ and $A_{ij}^s \equiv \mathbf{r}_{ij} \cdot \mathbf{A}^s$, respectively, with \mathbf{r}_{ij} ($|\mathbf{r}_{ij}| = a$ is equal to the lattice constant) a spatial vector connecting two NN sites, i and j . On the right-hand side (rhs) of the above expressions, $N^h(c)$ and $N_{\uparrow,\downarrow}^b(c)$ denote the numbers of holons and spinons of spin \uparrow or \downarrow , respectively, which are enclosed by an arbitrary counter-clockwise-oriented path c . Such a topological gauge structure *entangles* the otherwise decoupled spin and charge degrees of freedom and is called mutual duality since a spinon sees a holon as a π flux tube and *vice versa*, which has been also formulated in the path-integral formalism as a mutual Chern-Simons gauge theory³² with both time-reversal and spin rotational symmetries retained.

The phase string model with the mutual duality gauge structure can lead to a global phase diagram at low-doping as summarized²⁸ in Fig. 1. It has been shown³⁴ that as the temperature is reduced below the characteristic temperature T_0 of the UPP, the spins in the background start to form singlet pairs (bosonic RVB pairs) and condense, which is characterized by the RVB order parameter Δ^s . The short-range AF correlations simultaneously begin to grow below T_0 , in contrast to much weaker spin correlations above T_0 .

Several low-temperature phases, including the so-called LPP, which is also known as the SVP, the d-wave superconducting phase, and the AF phase at low doping, are all nested below the UPP as shown in Fig. 1 with essentially the *same* symmetry in the spin sector as characterized by Δ^s . The competitions between these low-temperature phases are basically decided by the above mutual-duality (mutual Chern-Simons) gauge structure, rather than more conventional competitions between different order parameters.

In particular, the LPP corresponds to the occurrence of holon Bose-condensation $\langle h_i^\dagger \rangle \neq 0$ without superconducting phase coherence, whose region is shaded in Fig. 1 and will be the main focus of the following study in this paper.

B. Superconducting order parameter

The LPP is the holon condensed phase on a background where spins form the singlet pairing. In order to understand the corresponding physical characteristics, it is instructive to examine the superconducting order parameter $\Delta_{ij}^{\text{SC}} = \sum_{\sigma} \langle c_{i\sigma} c_{j-\sigma} \rangle$ below.

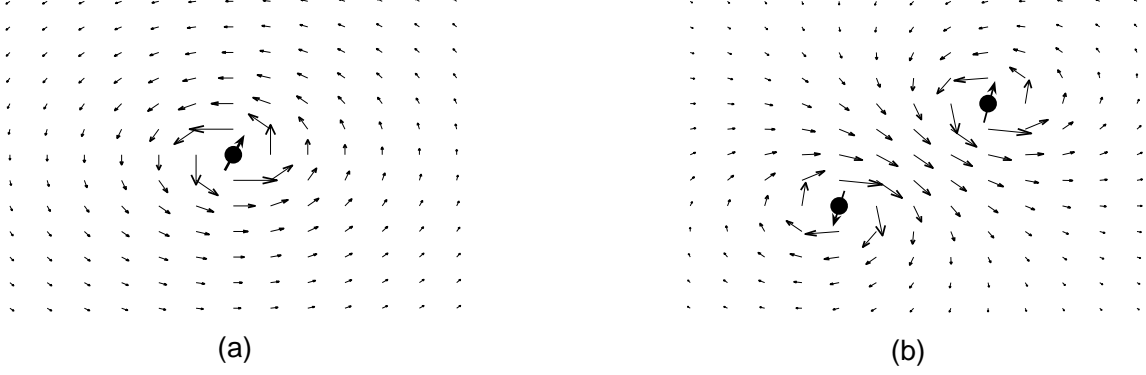


FIG. 2: (a) An isolated spinon is always associated with a 2π vortex in the phase of the superconducting order parameter in the phase string model. (b) A pair of vortex-antivortex with spinons located at the cores.

Based on the phase string formulation [Eq. (1)], the spinon RVB pairing [Eq. (5)], and the holon condensation condition $\langle h_i^\dagger \rangle \neq 0$, the superconducting order parameter defined at the NN sites can be expressed as³⁷ $\Psi_{\text{SC}} \equiv (\Delta_{ij}^{\text{SC}})_{\text{NN}} = \Delta_{ij}^0 \langle e^{i\frac{1}{2}(\Phi_i^s + \Phi_j^s)} \rangle$ where $\Delta_{ij}^0 \propto \sum_{\sigma} \langle e^{-i\sigma A_{ij}^h b_{i\sigma} b_{j-\sigma}} h_i^\dagger h_j^\dagger \rangle_{\text{NN}} \simeq \Delta^s \langle h_i^\dagger \rangle \langle h_j^\dagger \rangle \neq 0$. Since in the later GL description we shall treat the charge condensate in terms of a slowly varying continuous field, $\langle h_i^\dagger \rangle \rightarrow \psi_h^*(\mathbf{r}_i)$, it is convenient to rewrite Ψ_{SC} in the continuum limit (without considering the d-wave symmetry of the relative coordinate for simplicity) as follows

$$\Psi_{\text{SC}} \propto \Delta^0 \langle e^{i\Phi^s(\mathbf{r})} \rangle \quad (9)$$

where the amplitude

$$\Delta^0 = \Delta^s (\psi_h^*)^2 \quad (10)$$

and the phase $\Phi^s(\mathbf{r}_i) = \Phi_i^s$ is given by

$$\Phi^s(\mathbf{r}) = \int d^2\mathbf{r}' \text{Im} \ln [z - z'] [n_{\uparrow}^b(\mathbf{r}') - n_{\downarrow}^b(\mathbf{r}')] \quad (11)$$

with $n_{\sigma}^b(\mathbf{r}_i) \equiv n_{i\sigma}^b/a^2$.

Therefore, in the phase string model the superconducting order parameter Ψ_{SC} has an intrinsic *composite* structure of amplitude and phase components in Eq. (9). Here the Cooper pair amplitude Δ^0 is composed of the RVB pairing Δ^s and holon condensate ψ_h^* , which is finite at $T \leq T_v$ [note that generally $T_v < T_0$, as $\psi_h \neq 0$ is always underpinned by the spin singlet pairing in the present work (*cf.* Sec. III C)]. Thus the LPP can be physically regarded as the formation of the Cooper pair amplitude $\Delta^0 \neq 0$.

However, the onset of Δ^0 does not lead to superconductivity immediately. From Eq. (11), it is clear that Φ^s describes 2π phase vortices whose cores are centered at spinons: *i.e.*, $\Phi^s \rightarrow \Phi^s \pm 2\pi$ or $\Psi_{\text{SC}} \rightarrow \Psi_{\text{SC}} e^{\pm 2\pi i}$ each time as the coordinate \mathbf{r} continuously winds around a *spinon* once according to Eq. (11). In other words, a spinon is always associated with a 2π vortex in Ψ_{SC} , known as a *spinon-vortex composite* which is schematically illustrated in Fig. 2(a). A spinon-vortex and -antivortex pair of a finite range of separation will result in the cancellation of the phase Φ^s at a large length scale as shown in Fig. 2(b). Consequently, if there exist excited spinons freed from the RVB pairing, then Φ^s is generally disordered such that $\langle e^{i\Phi^s(\mathbf{r})} \rangle = 0$ and $\Psi_{\text{SC}} = 0$, which defines the LPP at $T_c < T < T_v$. Here the presence of *free* 2π vortices in the LPP is a direct manifestation of the electron “fractionalization”, *i.e.*, the existence of neutral $S = 1/2$ spinons in the underlying phase. In the opposite, the SC phase is determined by the phase coherence $\langle e^{i\Phi^s(\mathbf{r})} \rangle \neq 0$ which corresponds to the *spinon pair confinement* with no single spinon excitations allowed in the bulk of the sample in the Meissner phase. Thus, the LPP and the superconducting phase are very closely related, distinct mainly by a topological transition in the long-distance limit which is to be further discussed in Sec. III later.

Finally, we point out that a spin 1/2 bound to the core of a 2π vortex of the superconducting order parameter is a very general and natural consequence of doped Mott physics. Namely, with the depleting of superfluid (hole) density at the core center, due to the no double occupancy constraint, a spinon trapped inside is energetically most competitive. Generally there could be also two other ways to create topological excitations in the superconducting order parameter according to Eqs. (9) and (10), which correspond to a 2π -vortex singularity in the holon condensation order parameter $\psi_h(\mathbf{r})$ or the RVB order parameter Δ^s , respectively. However, the former vortex defined as $\psi_h(\mathbf{r}) \rightarrow \psi_h(\mathbf{r})e^{i\text{Im} \ln(z-z_0)}$ leads to a 4π vortex in Ψ_{SC} , which is energetically not favored. (Nevertheless, such 4π vortices do play a role when they are bound to the spinon vortices, as will be shown in Sec. II C.) The latter one does provide a 2π vorticity in Ψ_{SC} , but it costs an *expensive* core energy due to the suppression of the RVB pair order parameter, $\Delta^s \rightarrow 0$, at the vortex core. By comparison, Δ^s can still remain finite in the core of a spinon-vortex shown above, where the average $\langle e^{i\Phi_s(\mathbf{r})} \rangle$ is suppressed to zero within a scale defined by an intrinsic length scale of the unpaired spinon trapped inside. As to be shown later, the existence of spinon-vortices in the present theory provides a natural origin for “cheap” vortices in the LPP, with the core energy related to a characteristic spin gap scale.

C. Ginzburg-Landau equation

According to the above definition, the LPP represents a state of matter characterized by an order parameter field $\psi_h(\mathbf{r})$, on top of the bosonic RVB condensate, whose microscopic definition is given by

$$\psi_h(\mathbf{r}) = \langle h(\mathbf{r}) \rangle \quad (12)$$

where $h(\mathbf{r})$ is the continuum version of the bosonic holon matter field experiencing the Bose condensation. Different from an ordinary thermodynamic phase like the BCS superconducting state, in which the order parameter is expressed in terms of the electron operators (*i.e.*, a pair of the electron creation or annihilation operators), the holon operator $h(\mathbf{r})$ cannot be simply expressed based on a local combination of the electron operators. The corresponding off diagonal long range order (ODLRO) as suggested by Eq. (12): $\langle h^\dagger(\mathbf{r})h(\mathbf{r}') \rangle \rightarrow \psi_h^*(\mathbf{r})\psi_h(\mathbf{r}')$ at $|\mathbf{r} - \mathbf{r}'| \rightarrow \infty$, must be then a “hidden” ODLRO, meaning that it involves a nonlocal, infinite-body order parameter if to be expressed in terms of the electron operators. More profoundly, since $\psi_h(\mathbf{r})$ will couple to an internal gauge field whose symmetry cannot be spontaneously broken, the onset of Eq. (12), or more precisely, its amplitude (see below), should actually represent a crossover rather than a true phase transition.

In the following we introduce an effective GL description of the LPP based on the order parameter ψ_h . Let us start with the continuum version of Eq. (6) which is given by

$$H_h = \frac{1}{2m_h} \int d^2\mathbf{r} h^\dagger(\mathbf{r}) (-i\nabla - \mathbf{A}^s - e\mathbf{A}^e)^2 h(\mathbf{r}) \quad (13)$$

where $m_h = (2t_h a^2)^{-1}$ and \mathbf{A}^e is the electromagnetic vector potential which is seen solely by the holons which carry charge $+e$. By noting that the holons here are hard-core bosons with repulsive short-range interaction, one may generally write down the corresponding GL free energy $F_h = \int d^2\mathbf{r} f_h$ where³⁷

$$f_h = f_h^0 + \alpha |\psi_h|^2 + \frac{\eta}{2} |\psi_h|^4 + \frac{1}{2m_h} \psi_h^* (-i\nabla - \mathbf{A}^s - e\mathbf{A}^e)^2 \psi_h \quad (14)$$

with f_h^0 denoting the “normal state” free energy density. In the absence of fields and gradients in Eq. (14), the minimum of $f_h = f_h^0 + \alpha |\psi_h|^2 + \frac{\eta}{2} |\psi_h|^4$ gives rise to

$$|\psi_h|^2 = -\frac{\alpha}{\eta} \equiv \rho_h^0$$

at $\alpha < 0$. Here ρ_h^0 represents a bare “superfluid” density, which is assumed to remain finite throughout LPP and is reduced to a renormalized $\rho_h = |\psi_h|^2$ in the presence of \mathbf{A}^s .

By minimizing F_h , a nonlinear Schrödinger equation or differential GL equation satisfied by $\psi_h(\mathbf{r})$ can be obtained

$$\alpha\psi_h + \eta|\psi_h|^2\psi_h + \frac{1}{2m_h} (-i\nabla - \mathbf{A}^s - e\mathbf{A}^e)^2 \psi_h = 0 \quad (15)$$

with the standard “supercurrent” density given by

$$\mathbf{J}(\mathbf{r}) = -\frac{i}{2m_h} [\psi_h^*(\mathbf{r})\nabla\psi_h(\mathbf{r}) - \nabla\psi_h^*(\mathbf{r})\psi_h(\mathbf{r})] - \frac{\mathbf{A}^s + e\mathbf{A}^e}{m_h} \psi_h^*(\mathbf{r})\psi_h(\mathbf{r}) . \quad (16)$$

These equations are similar to an ordinary GL theory describing a charge $+e$ Bose condensate coupled to an external electromagnetic field \mathbf{A}^e , except that ψ_h is further coupled to the spin degrees of freedom through the vector potential \mathbf{A}^s , whose gauge-independent definition is given in Eq. (8). It means that each isolated spin (spinon) will register as a $\pm\pi$ flux tube in the nonlinear Schrödinger equation (15) to exert frustration effect on the charge condensate, which reflects the key influence of the spin degrees of freedom on the charge condensate in the phase string model.

The GL equations, Eqs. (15) and (16), are gauge invariant under the transformation: $\psi_h \rightarrow \psi_h e^{i\varphi}$ and $\mathbf{A}^s \rightarrow \mathbf{A}^s + \nabla\varphi$ where φ is an arbitrary single-valued function. Especially, one may also construct a *large* gauge transformation $\varphi = \sum_i \varphi_i$, with

$$\oint_{c_i} d\mathbf{r} \cdot \nabla\varphi_i = \pm 2\pi \quad (17)$$

where a loop c_i encircles a $\pm 2\pi$ vortex center i which coincides with a spinon position. This procedure is allowed because in the underlying microscopic theory a holon cannot stay at the sites of spinons due to the no double occupancy constraint and ψ_h should thus vanish at a spinon position where a $\pm\pi$ flux tube is bound to according to Eq. (8) (\mathbf{A}^s diverges there). Through such kind of large gauge transformation, the rhs. of Eq. (8) (if one spinon is enclosed by c) may be properly transformed by a minus sign as

$$\oint_c d\mathbf{r} \cdot \mathbf{A}^s = \pm\pi \rightarrow \oint_c d\mathbf{r} \cdot \mathbf{A}^s = \mp\pi \quad (18)$$

which means the sign of vorticity around a spinon is no longer directly tied to the spin index $\sigma = \uparrow, \downarrow$. In this way the theory is expressed in an explicitly spin-rotational invariant form, where the sign of the π fluxoid carried by each spin excitation (spinon) can be determined by minimizing the free energy instead.

The above large gauge transformation can be also visualized based on the superconducting order parameter Ψ_{SC} defined in Eq. (9). Evidently, Φ^s is related to \mathbf{A}^s ($\nabla\Phi^s = 2\mathbf{A}^s$), satisfying the gauge invariance under the gauge transformation: $\psi_h \rightarrow \psi_h e^{i\varphi}$, $\mathbf{A}^s \rightarrow \mathbf{A}^s + \nabla\varphi$, and $\Phi^s \rightarrow \Phi^s + 2\varphi$. If one makes *large* gauge transformations like Eq. (17), then the vorticity signs of the 2π vortices in Φ^s can be changed such that $n_{\uparrow}^b(\mathbf{r})$ and $n_{\downarrow}^b(\mathbf{r})$ generally should be replaced by

$$\Phi^s(\mathbf{r}) = \int d^2\mathbf{r}' \text{Im} \ln [z - z'] [n_{-}^b(\mathbf{r}') - n_{+}^b(\mathbf{r}')] , \quad (19)$$

where $n_{\pm}^b(\mathbf{r})$ denotes excited spinon number with vorticity $\pm 2\pi$ no longer be directly tied to the spin index (the definition of \pm sign for the vorticity is such that $+$ vortices are commensurate with the magnetic field applied along the perpendicular direction of the 2D plane, *cf.* Sec. III B). In order words, although $(\psi_h^*)^2$ only contributes 4π vortices to Ψ_{SC} , it can also change the sign of 2π vortices in Φ^s if the vortex cores of these 4π vortices *properly* coincide with the spinons (note that the higher vorticities like 6π per spinon as the result of the above transformation will cost too much energy and are thus not considered here).

In summary, the LPP phase is described by a generalized GL description of the holon condensate coupled with unbound spinon-vortices, the dynamics of which is governed by the spinon Hamiltonian (4). In the next section, the physical properties of the LPP phase will be explored based on such an effective description.

III. PHYSICAL PROPERTIES OF LOWER PSEUDOGAP PHASE

Let us first focus on the spin degrees of freedom below, which will play an important role in the LPP.

A. Spin degrees of freedom: A spin liquid

Let us recall that the spinon mean-field Hamiltonian (4) can be diagonalized by the following Bogoliubov transformation³⁰

$$b_{i\sigma} = \sum_m w_{m\sigma}(\mathbf{r}_i) \left[u_m \gamma_{m\sigma} - v_m \gamma_{m-\sigma}^\dagger \right] \quad (20)$$

with $u_m = 1/\sqrt{2}(\lambda/E_m + 1)^{1/2}$ and $v_m = 1/\sqrt{2}(\lambda/E_m - 1)^{1/2} \text{sgn}(\xi_m)$. The diagonalized Hamiltonian is written as

$$H_s = \sum_{m\sigma} E_{m\sigma} \gamma_{m\sigma}^\dagger \gamma_{m\sigma} + \text{const.} \quad (21)$$

where the spinon spectrum $E_m = \sqrt{\lambda^2 - \xi_m^2}$ and ξ_m is the eigenvalue of a tight-binding equation

$$\xi_m w_{m\sigma}(\mathbf{r}_i) = -J_s \sum_{j=NN(i)} e^{-i\sigma A_{ji}^h} w_{m\sigma}(\mathbf{r}_j) \quad (22)$$

Here the gauge field A_{ij}^h is constrained to the hole number according to Eq. (7), which incorporates the most nontrivial doping effect on the spin degrees of freedom in the phase string model. In the LPP when holons are Bose condensed, A_{ij}^h may be treated as describing a uniform flux of strength $\delta\pi$ per plaquette.

A spinon excitation created by $\gamma_{m\sigma}^\dagger$ with an eigen-energy E_m has no direct gauge coupling with the external electromagnetic field \mathbf{A}^e in the mean-field spinon Hamiltonian H_s [Eq. (21)] and is thus a charge-neutral, $S = 1/2$ object. Here a magnetic field can still couple to spinons via the Zeeman energy, $-\mu_B B \sum_{i\sigma} \sigma n_{i\sigma}^b$. Adding this term to H_s will lead to a modified spinon spectrum in Eq. (21)

$$E_{m\sigma} = E_m - \sigma \mu_B B \quad (23)$$

In obtaining Eq. (23) one need to note that

$$\sum_{i\sigma} \sigma n_{i\sigma}^b = \sum_{m\sigma} \sigma n_{m\sigma}^\gamma \quad (24)$$

with using $u_m^2 - v_m^2 = 1$ and $\sum_i |w_{m\sigma}(\mathbf{r}_i)|^2 = 1$, where the excited spinon number $n_{m\sigma}^\gamma$ is defined by

$$n_{m\sigma}^\gamma \equiv \gamma_{m\sigma}^\dagger \gamma_{m\sigma}. \quad (25)$$

In the LPP, by treating A_{ij}^h as a vector potential for a *uniform* flux perpendicular to the 2D plane with the field strength $B^h = \frac{\pi\delta}{a^2}$, the spinon wave function $w_{m\sigma}(\mathbf{r})$ determined by Eq. (22) is characterized by a wavepacket of a typical size of the cyclotron length scale $a_c = 1/\sqrt{B^h}$, *i.e.*,

$$a_c = \frac{a}{\sqrt{\pi\delta}}. \quad (26)$$

The RVB pairing of spins described by H_s in Eq. (21) has the following mean-field form in the ground state³³

$$|\text{RVB}\rangle = C \exp \left(\sum_{ij} W_{ij} b_{i\uparrow}^\dagger b_{j\downarrow}^\dagger \right) |0\rangle$$

where the RVB amplitude $|W_{ij}| = \left| \sum_m \frac{v_m}{u_m} w_{m\sigma}^*(\mathbf{r}_i) w_{m\sigma}(\mathbf{r}_j) \right|$ behaves as follows

$$|W_{ij}| \propto e^{-|\mathbf{r}_i - \mathbf{r}_j|^2 / 2\xi_s^2}$$

at $|\mathbf{r}_i - \mathbf{r}_j| \gg a$, for ij belonging to different sublattices. Here the characteristic size for the RVB pair is given by³³

$$\xi_s = a \sqrt{\frac{2}{\pi\delta}} \quad (27)$$

which also decides the equal-time spin-spin correlation length. Note that ξ_s diverges at small δ where an AFLRO emerges. Namely, the spin sector is described by a *spin liquid* at finite doping, which can be continuously connected to the AFLRO state as the doping concentration is reduced to zero.

Thus, although there exist a lot of spins at low doping ($1 - \delta$ per site), the majority of them form short-range RVB pairs of a typical size ξ_s in the holon condensation phase. According to Eq. (8), then the contribution of these RVB paired spins to \mathbf{A}^s will be effectively cancelled out, and the charge condensate described by ψ_h is essentially decoupled from the RVB background at a scale larger than ξ_s . This is also self-consistent with the fact that ξ_s is compatible with the average holon-holon distance which sets a minimal length scale for the holon condensate. Only the excited spinons will then effectively contribute to \mathbf{A}^s in the GL equation by noting that

$$\sum_{\sigma} \sigma \langle n_{i\sigma}^b \rangle = \sum_{m\sigma} \sigma |w_{m\sigma}(\mathbf{r}_i)|^2 \langle n_{m\sigma}^\gamma \rangle \quad (28)$$

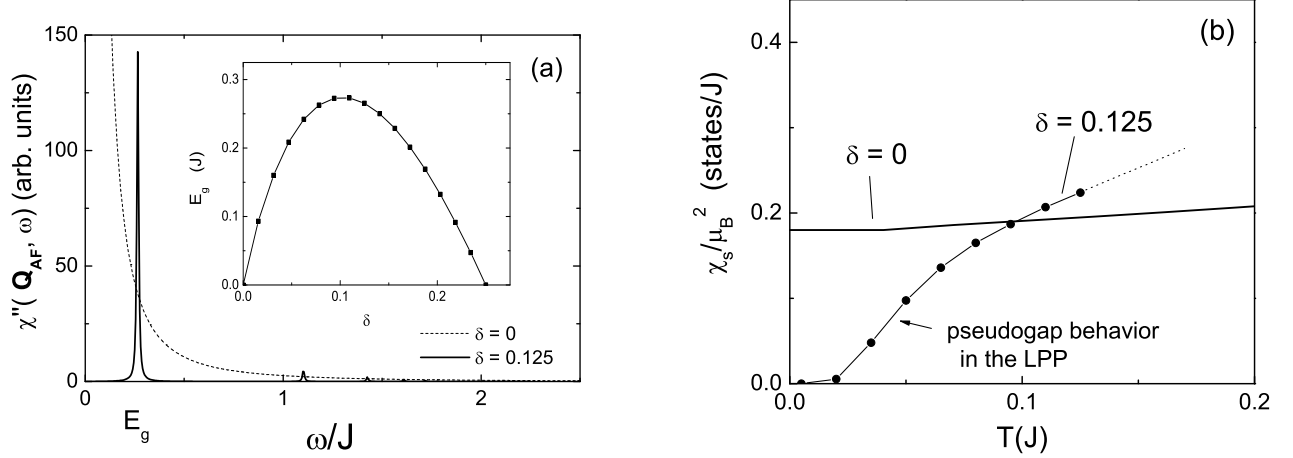


FIG. 3: Spin liquid behavior in the LPP at $\delta = 0.125$ as compared to the half-filling case with an AFLRO. (a) Dynamic spin susceptibility at momentum $\mathbf{Q}_{AF} = (\pi, \pi)$. Inset: the evolution of the resonancelike peak energy E_g as a function of doping concentration. (b) Uniform spin susceptibility versus the temperature.

based on the Bogoliubov transformation (20). In obtaining Eq. (28), one has used the fact that $|w_{m\sigma}(\mathbf{r})|^2$ is independent of σ . Here the length scale determined by $|w_{m\sigma}(\mathbf{r}_i)|^2$, *i.e.*, the “cyclotron” length a_c in Eq. (26) sets a natural spinon size which is within the “coarse graining” length ξ_s as $a_c = \xi_s/\sqrt{2} \lesssim \xi_s$. Thus an excited spinon can still maintain its quantum integrity in the GL equation description.

Eq. (21) describes the spinon excitations as neutral spin-1/2 excitations in the RVB background, labelled by m and spin index σ . Fig. 3(a) shows the corresponding dynamic spin susceptibility function at the AF wavevector $\mathbf{Q}_{AF} = (\pi, \pi)$ for $\delta = 0$ and $\delta = 0.125$, respectively, in which a resonancelike peak naturally emerges at finite doping. In the inset, such a resonance energy E_g as a function of doping is presented (the bare superexchange coupling J used in Ref.³⁵ should be replaced by a renormalized one J_{eff} in the expression of J_s as discussed in Ref.³⁴). Note that more precisely, the competing AF state can drive E_g vanish at $x_c \sim 0.04$ in a fashion of $E_g \sim \sqrt{\delta - x_c}J$,³¹ instead of $E_g \sim \delta J$ at $\delta \rightarrow 0$ as shown in Fig. 3(a), which is beyond the mean-field description presented here. In Fig. 3(b), the uniform spin susceptibility³⁴ is also shown for both $\delta = 0$ and $\delta = 0.125$, and the later one clearly exhibits a pseudogap behavior at low temperature. These typical magnetic properties evolving from the undoped AF phase to the LPP are quite consistent with the experimental measurements in the high- T_c cuprates.

B. Spin-charge entanglement in the LPP: Spinon-vortex composite

As discussed above, the spin sector in the LPP can be characterized as a spin liquid state with charge neutral, spin 1/2 spinons as its elementary excitations. Here one finds essentially the same symmetry for the spin degrees of freedom in both the UPP and LPP, which are described by the bosonic RVB order parameter Δ^s . What really differentiates the UPP and LPP lies in the charge sector by the additional holon condensation $\psi_h \neq 0$ in the LPP. As it turns out, this distinction in the charge degree of freedom then *feeds back* to the spin sector to affect the spin excitations, resulting in a spin gap behavior in the LPP as represented in Fig. 3 in the previous section.

In the following we shall discuss a more striking feature due to the mutual entanglement between the spin and charge degrees of freedom based on the GL equations. Namely, a spinon excitation will always induce a current vortex in the LPP to form a spinon-current-vortex composite, which is consistent with the 2π vortices previously identified in the phase of the superconducting order parameter in Sec. II B [Fig. 2(a)].

By writing

$$\psi_h = \sqrt{\rho_h} e^{i\phi_h} \quad (29)$$

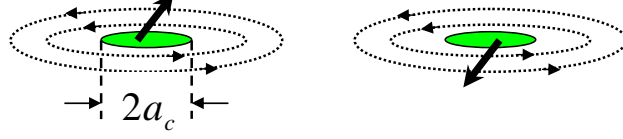


FIG. 4: A neutral spin-1/2 bosonic object, spinon, is always locking with a current vortex as an elementary excitation in the LPP, known as a spinon-vortex composite. The vortex core size is decided by the quantum length scale of the spinon, a_c , with its vorticity sign independent of the spin index.

a London equation for the supercurrent based on Eq. (16) (neglecting the spatial dependence of ρ_h) is given by

$$\mathbf{J}(\mathbf{r}) = \frac{\rho_h}{m_h} [\nabla\phi_h - \mathbf{A}^s - e\mathbf{A}^e] \quad (30)$$

Since each unpaired spinon will contribute to $\oint_c d\mathbf{r} \cdot \mathbf{A}^s = \pm\pi$ in terms Eq. (8) if the loop c encloses such a spinon of a typical radius of a_c , a *minimal* supercurrent vortex centered around it is then given by

$$\oint_c d\mathbf{r} \cdot \mathbf{J}(\mathbf{r}) = \pm\pi \frac{\rho_h}{m_h} \quad (31)$$

according to Eq. (30). This spinon-vortex composite is illustrated in Fig. 4, where the “cyclotron” length a_c serves as a natural radius for the core size of a spinon-vortex.

As discussed in Sec. II C, a large gauge transformation in ϕ_h can result in a binding of a 2π vortex to a spinon to change the sign of vorticity it carries. Consequently, a spinon excitation is always a composite of a neutral spin-1/2 locking with a charge current vortex in the LPP, but the vorticity and spin index are not necessarily the same. Such a spinon-vortex binding is a key consequence of holon condensation and play an essential role in understanding the LPP physics. Due to the presence of unconfined spinon-vortices, the LPP is a phase-frustrated BEC of holon and is more precisely characterized by the finite amplitude of ψ_h , $\sqrt{\rho_h}$.

By requiring that

$$\left\langle \oint_c d\mathbf{r} \cdot \mathbf{J}(\mathbf{r}) \right\rangle = 0$$

and omitting *independent* 2π vortices in $\nabla\phi_h$ (which are presumably important only at temperatures close to T_v), the following “neutrality” condition is then obtained

$$\begin{aligned} \oint_c d\mathbf{r} \cdot \mathbf{A}^e &= \frac{1}{e} \oint_c d\mathbf{r} \cdot (\nabla\phi_h - \mathbf{A}^s) \\ &= \phi_0 [N_+(c) - N_-(c)] \end{aligned} \quad (32)$$

where $\phi_0 \equiv hc/2e$ and $N_{\pm}(c)$ denotes the number of spinon-vortices (antivortices) enclosed in an arbitrary loop c . It shows that a perpendicular magnetic field will generally polarize the numbers of $\pm\pi$ spinon-vortices (the sign \pm is defined according to Eq. (32)) in the LPP.

Thus, spinon excitations in the LPP are no longer “free” ones solely determined by H_s in Eq. (21). They will actually acquire a long-range logarithmic interaction due to the spinon-vortex effect. Indeed, substituting Eq. (29) into Eq. (14) and carrying out the area integration, one finally obtains

$$F_h = \int \int d^2\mathbf{r}_1 d^2\mathbf{r}_2 \left[\sum_{\alpha} \alpha n_{\alpha}^b(\mathbf{r}_1) \right] V(\mathbf{r}_{12}) \left[\sum_{\beta} \beta n_{\beta}^b(\mathbf{r}_2) \right] + \text{const.} \quad (33)$$

in which $\alpha, \beta = \pm$ refer to the signs of vorticities carried by spinons and

$$V(\mathbf{r}_{12}) = -\frac{\pi\rho_h}{4m_h} \ln \frac{|\mathbf{r}_1 - \mathbf{r}_2|}{r_c} \quad (34)$$

with $r_c \sim a$. Nevertheless, in the LPP where a substantial number of spinon-vortices is present, the long-range force in Eq. (33) will be screened such that spinon-vortices are not bound together, as opposed to the lower-temperature

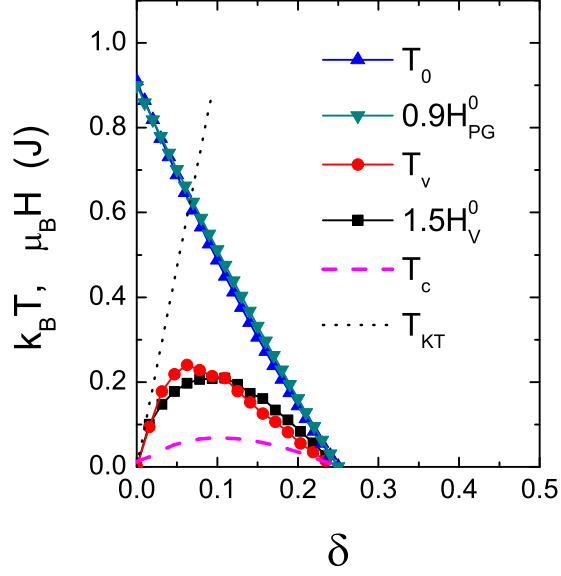


FIG. 5: The characteristic temperature and magnetic field scales which determine the phase diagram of the upper and lower pseudogap and superconducting phases based on the phase string model. Here T_0 and $H_{PG}^0 \equiv H_{PG}(T=0)$ for the UPP, T_v and $H_v^0 \equiv H_v(T=0)$ for the LPP, and T_c for the SC phase.

superconducting regime where all excited spinons form vortices-antivortices bound pairs (*cf.* Sec. III F). Namely the LPP remains an electron fractionalized state before it undergoes the superconducting phase transition at T_c .

However, in the LPP, the short-range interaction in Eq. (33) remains unscreened. Each excited spinon at a state labelled by m has a spatial extension determined by $|w_m(\mathbf{r})|^2$ as mentioned before. With involving the charge current, a symmetric profile of $|w_m(\mathbf{r})|^2$ in the symmetric gauge is energetically most favorable. Then a pair of spinon excitations at the same m with opposite vorticities have essentially no contribution from Eq. (33) due to the cancellation, but one with the same vorticities will cost a big repulsive core energy $\sim \frac{\pi \rho_h}{m_h}$ in F_h . Such a short-range interaction effect will be further considered later when we discuss the diamagnetism in the LPP.

C. Phase diagram

The phase diagram of the doped Mott insulator can be drawn by combining the description of the LPP phase here and the previous work on the UPP phase³⁴.

The upper pseudogap phase.—The phase string model holds for the whole bosonic RVB regime underpinned by $\Delta^s \neq 0$, which defines the UPP as illustrated in Fig. 1. The characteristic temperature T_0 and magnetic field H_{PG}^0 (at $T=0$) for the UPP at the boundary $\Delta^s=0$ have been previously determined in Ref.³⁴, which are consistent with the experimental measurements^{7,8,9,10}. Such temperature and magnetic field scales are replotted as functions of doping with $x_{RVB}=0.25$ in Fig. 5 (filled triangles).

The lower pseudogap phase.—Now let us consider the phase boundary of the LPP, which is set by vanishing ψ_h at T_v . Note that without \mathbf{A}^s this would be a simple 2D hard-core boson problem according to Eq. (13), and the KT temperature for the holon condensation is given by

$$T_{KT} = \pi \delta (2a^2 m_h)^{-1} \quad (35)$$

which has been previously used²³ as an upper bound temperature for the LPP at low doping, shown in Fig. 5 by a dotted line (with $t_h=3J$).

However, the frustration effect of \mathbf{A}^s on the holon condensation can be very important. The spinon-vortex density is determined by the density (per site) of spinon Bogoliubov quasiparticles as $n_v = \sum_{m\sigma} \langle n_{m\sigma}^\gamma \rangle / N$. Due to the opening up of a spin gap E_g in the holon condensation phase (*i.e.*, the LPP), n_v is exponentially small for $T \ll E_g$. With

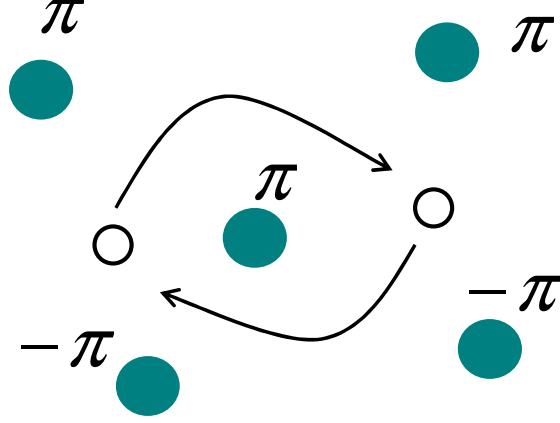


FIG. 6: Two holons (open circles) exchanging positions can pick up a minus sign if an unpaired spinon (grey circle) is enclosed in between, which carries a $\pm\pi$ flux tube due to the mutual duality gauge structure in the phase string model. So the phase coherence of bosonic holons can be effectively destroyed to prevent the Bose condensation if there is a sufficient number of free spinon excitations in the singlet spin background.

increasing temperature, n_v will monotonically increase until reaching the maximal number $n_v^{\max} = 1 - \delta$ at $T = T_0$ where all the RVB pairs break up.

Since each free spinon carries a π fluxoid as perceived by the holons, the quantum phase coherence among bosonic holons will be violently interrupted if on average there is an excited (unpaired) spinon sitting between each two neighbored holons (as illustrated by Fig. 6), where an exchange between a pair of holons can gain a minus sign in wavefunction. In other words, the holon condensation must break down when the vortex density n_v is comparable to holon density δ , far less than n_v^{\max} at low doping. Such a consideration provides an estimate of the upper bound for T_v as

$$n_v = \frac{1}{N} \sum_{m\sigma} \frac{1}{e^{E_{m\sigma}/k_B T_v} - 1} = \delta \quad (36)$$

T_v determined by Eq. (36) is plotted in Fig. 5 by filled circles (with $E_{m\sigma}$ determined by the self-consistent mean-field theory³⁴ of the UPP as $\psi_h \rightarrow 0$). Eq. (36) can be also understood based on the “core touching” picture of spontaneously excited spinon vortices in the LPP⁴⁶. Note that the average distance between excited spinons may be defined by $l_s \equiv 2a/\sqrt{\pi n_v}$. Since the characteristic core size of a spinon-vortex is $2a_c$ as shown in Fig. 4, then one expects that the “supercurrents” carried by spinon-vortices are totally destroyed when the sample is fully packed by the “cores” with $l_s = 2a_c$ which results in Eq. (36). Here it is emphasized that there is no simple mean-field phase transition for the LPP due to the peculiar mutual duality gauge structure mediated by \mathbf{A}^s and \mathbf{A}^h . Furthermore, 2π vortices of ψ_h , independent of spinon-vortices, will be also generally present near T_v as $\rho_h \rightarrow 0$. All of these fluctuation effects can affect the crossover from the LPP to UPP in details.

Similar to the UPP case³⁴, an external magnetic field will break up some RVB pairs through the Zeeman effect to create more excited spinons at a given temperature. By considering the Zeeman effect on the energy spectrum $E_{m\sigma}$ in Eq. (23), the magnetic field dependence of $T_v = T_v(H)$ can be further obtained from Eq. (36). Or conversely, for each $T < T_v$ there is a characteristic field $H_v(T)$ at which the LPP phase is destructed. $H_v^0 \equiv H_v(T = 0)$ determined this way is shown in Fig. 5 (filled squares). Roughly we find $k_B T_v \sim 1.5 \mu_B H_v^0$ according to Fig. 5, or $H_v^0/T_v \sim 0.99$ (T/K) which is slightly larger than the experimental ratio ~ 0.62 (T/K) determined by the Nernst measurement²⁰ in the LSCO compound. Furthermore, H_v as a function of temperature is further shown in Fig. 7 at doping concentration $\delta = 0.125$ (in the same figure, the critical field $H_{PG}(T)$ for the UPP is also shown, which terminates at $T = T_0$).

Superconducting phase.—The superconducting phase transition (the dashed curve in Fig. 5) is given by³⁸

$$T_c \simeq \frac{E_g}{4k_B} \quad (37)$$

which is determined by the characteristic energy E_g of the low-lying spin excitation—the so-called resonancelike peak

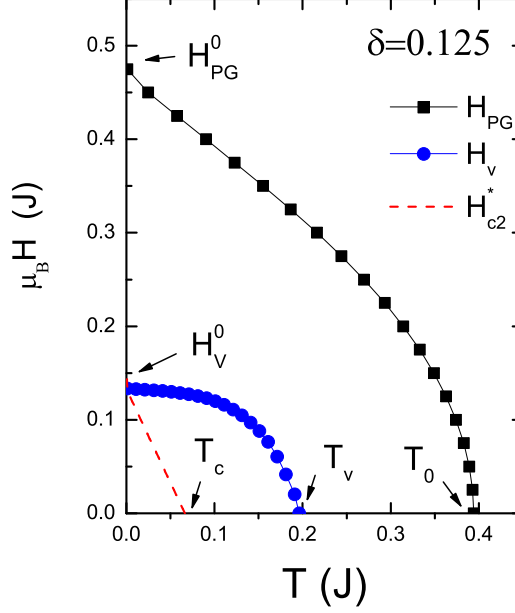


FIG. 7: The magnetic field – temperature phase diagram of the pseudogap phases at doping $\delta = 0.125$.

energy (*cf.* Fig. 3). Such a transition is non-BCS-like and is represented by a topological transition related to the phase coherence of the superconducting order parameter, which will be further discussed in Sec. III F.

In the mixed state below T_c , by including the Zeeman energy according to Eq.(23), E_g is reduced to $E_g^* = E_g(B) - 2\mu_B B$ such that one can estimate $T_c(B)$ by using a simple relation $T_c(B) \sim E_g^*/4k_B$. Then in turn one may define $H_{c2}^* \equiv B(T_c)$, which is shown in Fig. 7 by a dashed curve (here a self-consistent mean-field solution of E_g^* in the LPP, in the presence of the Zeeman term, is numerically determined). Note that H_{c2}^* so defined will vanish at T_c , resembling the conventional H_{c2} in a BCS superconductor. However, since free spinon-vortices are generally present at $H > H_{c2}^*$, H_{c2}^* is a crossover field which no longer has the same meaning as H_{c2} in the conventional BCS superconductor. Roughly speaking, the Abrikosov magnetic vortices (their total number is proportional to the magnetic field) are expected to be present below H_{c2}^* where the additional spinon-vortices generated by the Zeeman effect, with both signs in the vorticity, are still loosely paired, while the vortices unbinding occurs above H_{c2}^* . So H_{c2}^* defines a crossover between two types of vortex regime. Of course, if the Abrikosov vortex lattice are melt below H_{c2}^* , the distinction between the two vortex liquid regimes should be further blurred at H_{c2}^* . At $T = 0$, $H_{c2}^*(0)$ obtained by setting $E_g^* = 0$ is found to be numerically quite close to H_V^0 at $\delta = 0.125$ (Fig. 7), although there is no physical reason for them to be the same. The numerical result also shows that $\mu_B H_{c2}^*(0) \simeq E_g(B=0, T=0)/2$, or

$$H_{c2}^*(0) \simeq 3T_c \left(\frac{T}{K} \right) \quad (38)$$

according to Eq. (37) which is in quantitatively agreement with the critical magnetic field extrapolated from the specific heat measurement⁴⁷ in the SC phase by fitting the Volovik \sqrt{B} term of a d-wave superconductor in the presence of a perpendicular magnetic field.

Therefore, the LPP is distinct from the UPP by an additional charge condensation, and the former is always nested inside the latter because, in order to realize the condensation in the charge sector, the excited spinon-vortex density should be restricted to avoid too strong the frustrations on the former—each unpaired (excited) spinon always exerts destructive phase interference on the charge condensate in a form of carrying a π flux tube. Here one clearly sees how the mutual duality of the gauge structure plays a crucial role in fixing the phase boundary. Finally, a three-dimensional phase diagram of the UPP, LPP and SC phase in the parameter of magnetic field, doping concentration, and the temperature determined by the above methods is summarized in Fig. 8.

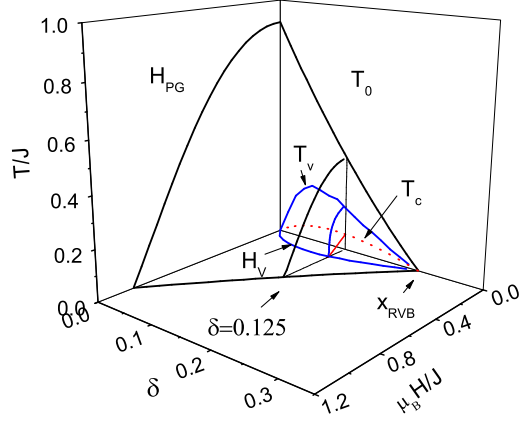


FIG. 8: The phase diagram of the pseudogap regimes in the three-dimensional space of magnetic field, doping, and temperature.

D. Nernst effect

In the absence of the integrity of fermionic quasiparticles (see Sec. III F), the transport properties in the LPP are mainly associated with the motion of spinon-vortices. This kind of transport is drastically different from the usual normal state transport contributed by quasiparticles, which more resembles that in the flux-flow phase of a BCS superconductor. But there are some crucial distinctions between the latter and the LPP. In a conventional type II superconductor, the vortex core energy is usually very large compared to the temperature $T \sim T_c$, which means that the thermal fluctuations of vortices can be ignored and nearly all the vortices are generated by an external magnetic field such that $n_v = B/\phi_0$. On the opposite, in the present LPP, the spinon-vortices as quantum objects can be created thermally, which means $n_v \gg B/\phi_0$ in weak field case. It is those *spontaneous* vortices that will decide the transport phenomenon in such a region.

Let us start with the charge current given by the London-like equation in Eq. (30). By using the steady current condition

$$\partial_t \mathbf{J} = 0 \quad (39)$$

and the definition of the electric field $\mathbf{E} = -\partial_t \mathbf{A}^e$ in the transverse gauge, one can finally obtain the following basic relation

$$\mathbf{E} = \hat{\mathbf{z}} \times \phi_0 (n_v^+ \mathbf{v}_+ - n_v^- \mathbf{v}_-) \quad (40)$$

where n_v^\pm denotes the density of spinon-vortices and -antivortices with drifting velocity \mathbf{v}_\pm along a direction perpendicular to the electric field in the plane. As illustrated by Fig. 9(a), the electric field and the drifting of vortices and antivortices must be balanced according to Eq. (40) in order to avoid the system being accelerated indefinitely ($\partial_t \mathbf{J} \neq 0$). So the applied electric field will drive the vortices and antivortices moving along a perpendicular direction with opposite velocities: $\mathbf{v}_+ = -\mathbf{v}_-$ if the vortices and antivortices are not polarized by the external magnetic field, *i.e.*, $n_v^+ = n_v^-$. Equation (40) is a basic relation for the spinon-vortex-related transport phenomenon in the LPP.

The Nernst signal corresponds to the electric field measured along the \hat{y} -direction when spinon-vortices and -antivortices are both driven by a temperature gradient in the *same* direction along the \hat{x} -direction. Such a case is shown in Fig. 9(b), where the spinon-vortices and -antivortices move along the \hat{x} -direction with the same velocity $\mathbf{v}_+ = \mathbf{v}_- = \mathbf{v}$ in a steady state. To have a finite \mathbf{E} in terms of Eq. (40), then the vortex density n_v^\pm has to be polarized by the external magnetic field $\mathbf{B} = B\hat{\mathbf{z}}$ according to the “neutrality” condition (32):

$$B = \phi_0 (n_v^+ - n_v^-) \quad (41)$$

such that

$$\mathbf{E} = \hat{\mathbf{z}} \times \phi_0 (n_v^+ - n_v^-) \mathbf{v} = \mathbf{B} \times \mathbf{v}$$

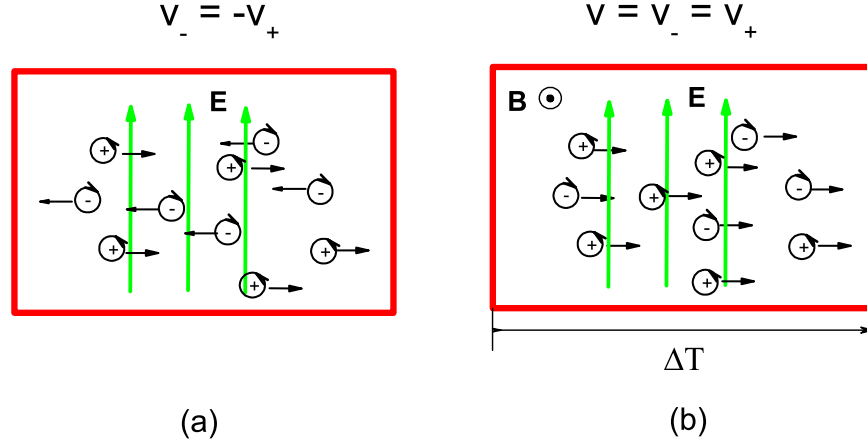


FIG. 9: Schematic picture of (a) the flux flowing under an electric field in the LPP, which can lead to a flux flow resistivity as well as the spin Hall effect, and (b) the flux flowing under a temperature gradient ∇T , which must be balanced by an electric field E and thus leads to the Nernst effect.

Define the Nernst signal e_N by

$$e_N = \frac{E_y}{-\nabla_x T} . \quad (42)$$

Suppose s_ϕ is the *transport* entropy carried by a spinon vortex and η_s is its viscosity such that the drift velocity \mathbf{v}^s can be decided by $s_\phi \nabla T = -\eta_s \mathbf{v}$. Then one has

$$e_N = B \frac{s_\phi}{\eta_s} \quad (43)$$

On the other hand, in the absence of the temperature gradient, a charge current can also drive a transverse motion of spinon-vortices and -antivortices along *opposite* directions, i.e., $\mathbf{v}_\pm = \pm \mathbf{v}$, such that an electric field is generated along the current direction according to Eq. (40), leading to a finite resistivity due to the presence of free vortices, which is given by⁴⁸

$$\rho = \frac{n_v}{\eta_s} \phi_0^2 \quad (44)$$

where

$$n_v \equiv n_v^+ + n_v^-$$

denotes the total density of vortices and antivortices. This formula is familiar in the vortex flow regime of a conventional superconductor. Then, by eliminating η_s which is harder to calculate, one obtains

$$\begin{aligned} \alpha_{xy} &\equiv \frac{e_N}{\rho} \\ &= \frac{B s_\phi}{\phi_0^2 n_v} \end{aligned} \quad (45)$$

where α_{xy} is the quantity introduced in Ref.¹⁵. It is noted that in the vortex phase of a conventional superconductor, one has $B = \phi_0 n_v^+ = \phi_0 n_v$ with $n_v^- = 0$ such that Eq. (45) reduces to $\alpha_{xy} \phi_0 = s_\phi$ from which the transport entropy

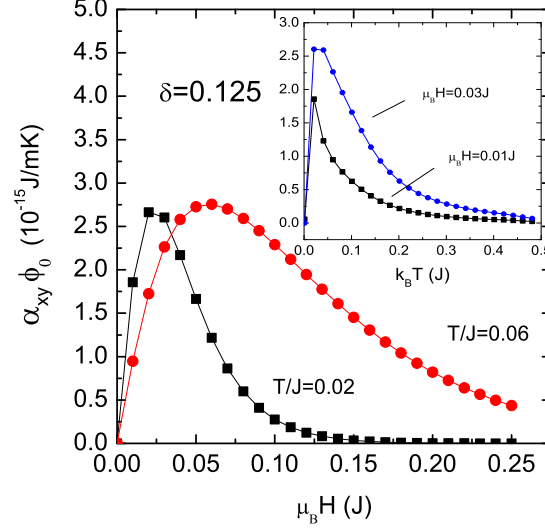


FIG. 10: The quantity $\alpha_{xy}\phi_0/d \equiv e_N\phi_0/\rho d$, which is related to the Nernst signal without involving the viscosity coefficient, is shown as a function of the magnetic field and temperature (the inset) at a given doping. Here $d = 7.7\text{\AA}$ is the distance between two CuO_2 layers.

of a vortex can be obtained directly (e.g., Ref.¹⁶). But in the LPP, $\alpha_{xy}\phi_0 = s_\phi(B/\phi_0 n_v) < s_\phi$, which means the transport entropy is underestimated by $\alpha_{xy}\phi_0$ here.

So far all the derivations are similar to the flux flow region in a conventional superconductor except that the total vortex number n_v in Eq. (45) generally is no longer simply proportional to the applied magnetic field B , which remains finite even in the limit $B \rightarrow 0$ to account for thermally activated spinon-vortices. What really makes the Nernst transport unique in the present theory is that the transport entropy s_ϕ here is due to the spin degree of freedom associated with a spinon-vortex, instead of a normal core in a conventional BCS superconductor. Let us recall that the core size of a spinon-vortex is determined by the “cyclotron” length scale a_c . If one neglects the “configuration” entropy associated with the spatial location of a spinon-vortex, then the main “transport entropy” as carried by a spinon-vortex is due to its free $S = 1/2$ moment which gives rise to

$$s_\phi = k_B \{ \ln [2 \cosh(\beta \mu_B B)] - \beta \mu_B B \tanh(\beta \mu_B B) \} . \quad (46)$$

Here the interaction between spinons in different vortex cores are ignored, which will in general lead to an additional suppression of the average entropy per vortex. Under such an approximation, $s_\phi \rightarrow 1/2$ for $T \gg \mu_B H$ and $s_\phi \rightarrow 0$ for $T \ll \mu_B H$. Despite of the saturation of s_ϕ at high temperature, the quantity α_{xy} defined in Eq. (45) decreases at high temperature due to the quick proliferation of the total vortex number. The temperature and magnetic field dependence of $\alpha_{xy}\phi_0/d$ is shown in Fig. 10, in which $d = 7.7\text{\AA}$ is the distance between two CuO_2 layers. The magnitude of such a quantity is quite comparable to the experimental data¹⁶, implying that the transport entropy due to the free moment in a spinon-vortex is capable to produce the Nernst signal observed experimentally. However, at strong magnetic field or high temperature, α_{xy} decays slower than that seen in the real systems. That is because here we have only considered single rigid spinon-vortices without taking into account the interaction between spinon-vortices as well as the fluctuations of vortices, which become very important as the LPP will eventually collapse at H_v and T_v as discussed before.

Finally, we briefly mention a unique prediction related to the spinon-vortex motion driven by an external electric field. As shown in Fig. 9(a), vortices can be driven by an in-plane electric field to move along the transverse direction. Since each vortex carries a free moment, if these moments are partially polarized, say, by an external magnetic field via the Zeeman effect, then a spin Hall current can be generated along the vortex motion direction. The spin Hall conductivity has been recently obtained⁴⁸ as follows:

$$\sigma_H^s = \frac{\hbar\chi_s}{g\mu_B} \left(\frac{B}{n_v\phi_0} \right)^2 \quad (47)$$

which only depends on the intrinsic properties of the system like the uniform spin susceptibility χ_s , with the electron g -factor $g \simeq 2$. It is important to note that the external magnetic field B applied perpendicular to the 2D plane reduces the spin rotational symmetry of the system to the conservation of the S^z component only, satisfying $\frac{\partial S^z}{\partial t} + \nabla \cdot \mathbf{J}^s = 0$. Thus the polarized spin current \mathbf{J}^s is still conserved and remains dissipationless as the *current* of its carriers – vortices is *dissipationless* in the LPP. In contrast, the charge current remains dissipative with the resistivity given by Eq. (44). The dissipationless spin Hall effect in the LPP is therefore an important prediction of the phase string model. For more details one is referred to Ref.⁴⁸.

E. Diamagnetism

In an ordinary superconductor, the diamagnetism can be well described in terms of the GL free energy. In such a description, the vortex phase below T_c , as induced by magnetic field, exhibits strong residual diamagnetism, continuously evolving from a perfect Meissner state and eventually vanishing as the magnetic field $H \rightarrow H_{c2}$ or temperature $T \rightarrow T_c$ when the Abrikosov vortices become closely packing (“core touching”). The diamagnetism here is directly connected to the energy cost for creating a vortex which carries swirling supercurrents and is subject to long-range interactions with other vortices, where the total number of vortices is usually proportional to the applied magnetic field by $n_v = B/\phi_0$.

The present LPP is a vortex liquid state *above* T_c , and it would be natural for one to conjecture that a substantial diamagnetism still persist. However, like the Nernst effect discussed above, due to the involvement of *spontaneous* vortices as well as the spin degrees of freedom, the theoretical description of the diamagnetism will be also modified drastically. In the present of thermal vortices, a weak magnetic field will mainly polarize the numbers of vortices and antivortices, instead of creating new vortices, and thus the diamagnetism due to the energy cost of the vortex creation will diminish quickly. On the other hand, if there is a dense population of thermal vortices, then the configuration entropy will sensitively depend on the imbalance of the numbers of vortices and antivortices, due to the “hard-core” like repulsion between two vortices of the same sign of vorticity as discussed before, which will cause an additional diamagnetism response.

Let us note that the total free energy for the LPP is given by

$$F = F_h + F_s + \int d^2\mathbf{r} \frac{B^2}{8\pi} \quad (48)$$

where B is the magnetic field perpendicular to the plane and F_s is the free energy for the spin part: $F_s = -\beta^{-1} \ln \text{Tr} (e^{-\beta H_s})$. The magnetization $M = (B - H)/4\pi$ is determined by

$$M = -\frac{1}{\Omega} \left(\frac{\partial F_h}{\partial B} + \frac{\partial F_s}{\partial B} \right)_T \quad (49)$$

where Ω denotes the 2D area of the system.

As discussed before, Eq. (49) is composed of two kinds of sources for diamagnetism. The first one is similar to that in the conventional vortex phase of a BCS superconductor contributed by supercurrents associated with vortices. But the vortex liquid phase *above* T_c is represented by the presence of a sufficient number of thermally excited free vortices that destroy the superconducting phase coherence. These spontaneous free vortices are already present in the absence of an external magnetic field perpendicular to the 2D plane, due to the screening of the long-range (logarithmic) interaction among vortices [Eq.(33)]. So in the vortex liquid phase, the free energy F , to the leading order approximation, should only depend on the total number n_v of vortices and antivortices, each with the same renormalized self-energy. On the other hand, when the applied magnetic field is weak enough as compared to the total number per unit area of thermally-excited vortices multiplying the flux quantum ϕ_0 (i.e., $B \ll n_v\phi_0$), it can only partially polarize the numbers of + and - vortices by Eq. (41): $\Delta n_v = B/\phi_0$, while the total vortex number n_v remains unchanged. Without an explicit dependence of F on the polarization Δn_v of vortices and antivortices that is proportional to the magnetic field, one would find a vanishing diamagnetic response to the weak magnetic field.

Another origin of diamagnetism is related to the entropy part of the free energy, as already pointed out above. In the following we provide an estimate of this effect as a *lower* bound of the diamagnetism at weak field limit. Recall that we have previously discussed the quantum mechanical nature of the core of a spinon-vortex: the trapped spinon

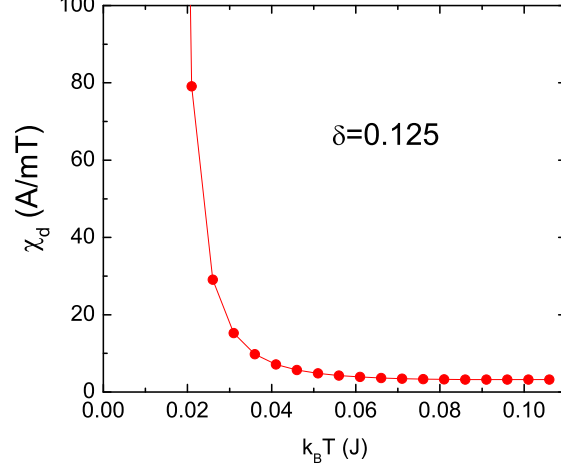


FIG. 11: The diamagnetic susceptibility versus temperature in the LPP.

does a cyclotron motion within the core according to H_s , and its Hilbert space is restricted to the lowest Landau level (LLL) at low temperatures ($\gtrsim T_c$). The above-mentioned short-range interactions will then dramatically affect the entropy of spinon-vortices: two vortices with the same vorticity will cost a large, unscreened energy if they stay in the same real-space (symmetric) cyclotron orbit labelled by m , whereas two with opposite vortices approximately do not experience any substantial short-range interaction even when they are in the same real-space orbit. Then we can approximately write down the total spinon-vortex configuration entropy as

$$S_s = \Omega k_B \sum_{\alpha} \left[n_{\alpha}^s \ln \left(\frac{G}{n_{\alpha}^s} - 1 \right) - g \ln \left(1 - \frac{n_{\alpha}^s}{G} \right) \right] \quad (50)$$

where N is the number of lattice sites and $N_{\alpha}^s = n_{\alpha}^s N$ is the spinon number with spin index α . $G = \delta/2 \times 2 = \delta$ denotes the degeneracy of the LLL per unit area, including the spin index, and the condition that two same vortices cannot occupy the same state labelled by m has been used with assumption that at $T \gtrsim T_c$ mainly the LLL is involved.

When the magnetic field is in the range of $B \ll n_v \phi_0$, one can reasonably assume $\delta B = \phi_0 (\delta n_v^+ - \delta n_v^-) = 2\phi_0 \delta n_v^+ = -2\phi_0 \delta n_v^-$ since $\delta n_v = \delta n_v^+ + \delta n_v^- \simeq 0$. Then, the magnetization determined by the entropy S_s is given as follows

$$\begin{aligned} M_s &\simeq \frac{T}{\Omega} \left(\frac{\partial S_s}{\partial B} \right)_{n_v} = \frac{T}{\Omega(2\phi_0)} \left(\frac{\partial S_s}{\partial n_v^+} \right)_{n_v} \\ &= \frac{k_B T}{2\phi_0} \ln \left(\frac{G - n_+^s}{G - n_-^s} \frac{n_-^s}{n_+^s} \right) \end{aligned}$$

At weak field limit, the rhs of the above expression may be expanded to the first order of B as

$$M_s = -\chi_d^0 B, \text{ or } M_s = \chi_d H$$

with

$$\chi_d = -\frac{\chi_d^0}{1 + 4\pi\chi_d^0} \quad (51)$$

where $\chi_d^0 = \frac{2Gk_B T}{(2G - n_v)n_v\phi_0^2}$. In Fig. 11, χ_d^0 is shown as a function of the temperature at $\delta = 0.125$, whose magnitude is comparable to the experimental result¹⁹ at $H = 1$ T. Note that at $T = 0$ one has $n_v = 0$ and $\chi_d^0 \rightarrow -\infty$ such that $M_s \rightarrow -(1/4\pi)H$, where the full Meissner state is recovered. In reality, one has $n_v = 0$ below T_c and thus expects to see a divergence in χ_d there. Near T_c the correction from the superconducting phase fluctuations may be important to result in some nonlinear singular field dependence¹⁹ of M_s which is not included in Eq. (51). Furthermore, χ_d

reaches a minimum but does not vanish at T_v where $n_v \sim \delta$ because the rigid spinon-vortices are considered here without taking into account of the collapse of spinon-vortices close to T_v . Finally, as remarked before, here we have only focused on the weak field limit $B \ll n_v \phi_0$. With increasing the magnetic field, more spinon-vortices will be generated and nonlinear effect at strong magnetic field will emerge which is explored quantitatively elsewhere⁴⁹.

F. Superconducting phase transition

With $\Delta^0 \neq 0$ in the LPP, the superconducting state can be finally realized through the phase coherence³⁷

$$\langle e^{i\Phi^s(\mathbf{r})} \rangle \neq 0 \quad (52)$$

in which the spinon-vortex composites must form vortex-antivortex pairs [*cf.* Fig. 2(b)] in an analog with the KT transition in the XY model.

The corresponding dynamics is decided by Eq. (33). It is similar to the XY model, except that \mathbf{A}^s introduces π instead 2π vortices and the vortex cores are attached to spinons which have their own dynamics as governed by H_s with an intrinsic quantum length scale a_c . Consequently the superconducting phase transition is not of a BCS-type second-order one as described by an ordinary GL theory — here ψ_h or more precisely the amplitude $\sqrt{\rho_h}$, is in general not expected to vanish at T_c , especially in the underdoped regime. It is rather a phase coherence transition involving spinon-vortices binding/unbinding which directly affects $e^{i\Phi^s(\mathbf{r})}$. The detailed renormalization group analysis³⁸ leads to the T_c relation (37) which connects the phase coherence temperature with the spin resonancelike energy E_g in a quantitative agreement with experimental measurements⁵⁰.

The superconducting phase coherence (52) implies that spinons are *confined* in the bulk where a single spinon-vortex excitation costs a logarithmically divergent energy. In this case, the low-lying elementary excitations are $S = 1$ spin excitations composed of pairs of spinon-vortices. Similar to the LPP, the spin resonancelike mode is basically composed of a pair of spinons with $E_g = 2E_s \sim \delta J_s$ with $E_s = (E_m)_{\min}$ denoting the lowest level in the spinon spectrum in terms of H_s in Eq. (21), which appears in the dynamic spin susceptibility at $\mathbf{Q}_{AF} = (\pi, \pi)$ as shown in Fig. 3(a) in the LPP. However, in the SC phase, the additional correction from Eq. (33) can modify such a low-lying mode by that for a pair of spinons with different m 's, the confinement force from F_h in Eq. (33) can further add a tail in the resonancelike peak from $2E_s$ towards higher energy.

Another stable elementary excitation in the SC phase is the quasiparticles composed of spinon-holon pairs as discussed in Ref.⁴¹. The d-wave nodal quasiparticle dispersion is schematically shown in Fig. 12, where the quasiparticle spectral function has a sharp lineshape below the spinon characteristic energy scale $E_s = E_g/2$ as energetically it cannot decay into a spinon and a holon in the condensation even *locally*. Above E_s , however, the composite (spin-charge separation) feature can show up in the lineshape of the spectral function, since energetically the quasiparticle can decay into a pair of spinon and holon *locally* without costing much from the logarithmic confining potential.

Therefore, at low energy and long-distance, there is no more electron fractionalization in contrast to the LPP. A single spinon-vortex composite can only emerge as a magnetic vortex core in the mixed state, where it ensures the minimal flux quantization at $\phi_0 \equiv hc/2e$ as discussed in Ref.³⁷. The phase string theory predicts that a free $S = 1/2$ moment must appear in the core of a Arbrikosov magnetic vortex, even though a Kondo screening effect due to the coupling to the background quasiparticles may complicate the analysis of possible experimental observations of such moments.

IV. SUMMARY AND CONCLUSIONS

In this paper, we have systematically explored the physical properties of the lower pseudogap phase in the phase string model. In the global phase diagram of the phase string model, the lower pseudogap phase corresponds to the regime where the amplitude of the superconducting order parameter becomes finite, but the order parameter itself is still short of phase coherence. The presence of free vortices in this phase prevents the system from undergoing superconducting until some lower temperature is reached where the vortices and antivortices form bound pairs. So the lower pseudogap phase and the superconducting phase are intimately related and the former sets a stage for the latter to emerge.

What makes the present microscopic theory really unique is that the above picture is naturally embedded in a spin-charge separation description. That is, for a doped Mott insulator, spin and charge correlations evolve distinctly, especially at low doping. Thus, at different energy/temperature scales, the spin and charge degrees of freedom play rather different roles. For example, at low doping and high temperature the neutral spins start to form the singlet pairing to lower the superexchange energy, which occurs at the expense of the kinetic energy of doped holes and the

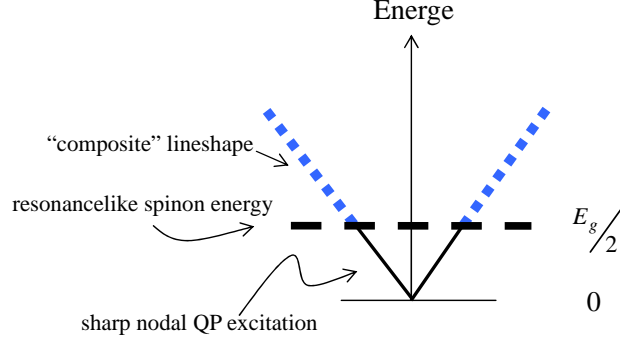


FIG. 12: A schematic nodal quasiparticle dispersion in the superconducting phase. The lineshape below the characteristic spinon energy $E_g/2$ is very sharp as energetically the quasiparticle cannot decay into a spinon and a holon in the condensate. Above $E_g/2$, however, such a decay is energetically allowed *locally* with the spinon and holon remain loosely confined at large distance.

latter behave quite incoherently in this upper pseudogap phase. So the spin correlations are the dominant driving force in this high-temperature pseudogap phase, where the antiferromagnetic fluctuations *continuously* increase with the decrease of the temperature, and would grow into a true long range order at zero temperature if there were no intervention from the charge degree of freedom at some lower temperature at finite doping.

However, the kinetic energy of holes would be highly frustrated in a long-range antiferromagnetically correlated spin background. Actually the kinetic energy will eventually win over the long-wavelength spin correlations beyond a small finite doping concentration at sufficiently low temperature (Fig. 1). In this regime the trend of growing antiferromagnetic fluctuations will get stopped and the system makes a crossover into the lower pseudogap phase at low temperature instead. Here the equal-time spin correlation length becomes truncated in the same order of magnitude as the average hole-hole distance [*cf.* Eq.(27)]. The corresponding spin gap behavior in the spin channel is clearly illustrated by the emergence of a resonancelike peak at energy E_g in the spin dynamic susceptibility at the antiferromagnetic wavevector in Fig. 3(a) and the suppression of the uniform spin susceptibility at low temperature in Fig. 3(b).

The spin liquid behavior in the lower pseudogap phase is thus the consequence of the competition between the charge and spin degrees of freedom, in which the kinetic energy of doped holes wins. Though suppressed in density, the thermally activated spin excitations across the spin gap can still exert frustration effect on the kinetic energy of doped holes as the reminiscence of the competition between the charge and spin sectors, which is the cause for the phase disordering. So the superconducting phase can be finally realized only when those spin excitations which bring destructive effect on the charge condensate are all excluded out of finite-energy spectra by some form of confinement.

Technically, in the phase string model represented by the effective Hamiltonians (4) and (6), the spin and charge degrees of freedom are mathematically characterized by *bosonic* spinon and holon fields, respectively, which are coupled together by a mutual duality gauge structure. These *bare* spinons form RVB pairs, and spinon excitations are the result of the broken RVB pairs. The lower pseudogap phase corresponds to the condensation of bosonic holons, which obviously is connected to the kinetic energy gain in the charge sector. The holon condensation then feedbacks to the spin sector to lead to the suppression of low-lying antiferromagnetic fluctuations and the opening of the spin gap through the topological gauge structure. The holon condensation is also self-consistently strengthened by this spin gap opening effect, because the fractionalized spin excitations—spinons carry fictitious π flux tubes as perceived by the holons and thus always introduce destructive phase interference for the latter.

In the lower pseudogap phase, even though the density of states get suppressed, spinons carrying π flux tubes still can be excited thermally across the energy gap $E_s = E_g/2$. It is well known that a π flux tube in a Bose condensate will always induce a vortexlike supercurrent response. That is precisely what happens in the lower pseudogap phase and each excited spinon is thus locking into a current vortex to form the spinon-vortex composite as shown in Fig. 4. Therefore the lower pseudogap phase is a vortex liquid/spin liquid phase, which is also known as the spontaneous vortex phase since these spinon-vortices can be thermally excited without involving external magnetic field.

So the central prediction of the present microscopic theory is the existence of spinon-vortices as elementary excitations in the LPP. A spinon-vortex plays a dual role here. On one hand, it carries a neutral spin-1/2 and indicates the spin-charge separation or electron fractionalization in the lower pseudogap phase. On the other hand, it is bound to a charge current vortex and contributes to a 2π phase vortex in the superconducting order parameter. The latter

property distinguishes the lower pseudogap phase from the upper pseudogap phase, and represents a mid-step towards the true spin-charge recombination, which is established in the superconducting phase where spinon-vortices are “confined” to form conventional $S = 1$ spin excitations and to result in coherent quasiparticle excitations by the holon-spinon confinement.

The vortex core of a spinon-vortex is distinctly different from a conventional vortex (like in the BCS superconductor). In the latter a competing “normal state” is nucleated at the core, whereas in the former an elementary fractionalized object, spinon, naturally serves as a core. These spinon-vortices are actually *always* present, even in the superconducting ground state where all of them are just paired up, instead of “*being annihilated*”. So to create a unpaired vortex at low energy/temperature, one only needs to break up an RVB pair without “nucleating” an additional “core”. To the leading order of approximation, the energy scale for creating a vortex is the spinon energy gap $E_s \sim \delta J$ at low doping. In this sense, the spinon-vortices are really “cheap” vortices which can be thermally (spontaneously) excited in the lower pseudogap phase. In a similar sense, the lower pseudogap phase is not a “competing” phase of essentially different symmetries with regard to the superconducting state. Rather the former is distinguished from the latter mainly in the long-wave length limit, much larger than the core size a_c and the RVB pairing size or equal-time spin correlation length, ξ_s , where the thermally excited spinon-vortices form vortex-antivortex pairs to realize the superconducting phase coherence.

Consequently the onset of the LPP at T_v or H_v , though a charge behavior, is determined by the spinon excitation according to Eq. (36), which can be understood based on the “core touching” picture of spinon vortices with the “supercurrents” being totally squeezed out. The Nernst effect has been also connected to the spin degrees of freedom as the latter provide transport entropy, while the diamagnetism in the low field limit is associated with the configurational entropy of spinon-vortices. The overall theoretical results are found to be in the correct magnitude as compared with the experimental measurements in the cuprates. Furthermore, a conserved, dissipationless spin Hall effect has been also predicated as a unique feature for the LPP. We shall present more detailed and quantitative results based on the mutual Chern-Simons gauge theory of the phase string model in a separate publication⁴⁹.

Acknowledgments

We would like to thank V. N. Muthukumar, S. P. Kou, Z. C. Gu, and W. Q. Chen for stimulating discussions and early collaborations. We also thank P. W. Anderson, N. P. Ong, D. N. Sheng, Y. Y. Wang, H. H. Wen, and F. C. Zhang for very helpful discussions. The authors acknowledge the support of the grants from the NSFC and MOE.

-
- ¹ For a review, *see*, T. Timusk and B. Statt, Rep. Prog. Phys. **62**, 61 (1999).
 - ² For a review, *see*, P. A. Lee, N. Nagaosa, and X.-G. Wen, Rev. Mod. Phys. (in press), cond-mat/0410445.
 - ³ K. Ishida, K. Yoshida, T. Mito, Y. Tokunaga, Y. Kitaoka, K. Asayama, Y. Nakayama, J. Shimoyama, and K. Kishio, Phys. Rev. B **58**, R5960 (1998).
 - ⁴ T. Watanabe, T. Fujii, and A. Matsuda, Phys. Rev. Lett. **84**, 5848 (2000).
 - ⁵ T. Timusk, Solid Stat. Commun. **127**, 337 (2003).
 - ⁶ Y. Ando, S. Komiya, K. Segawa, S. Ono, and Y. Kurita Phys. Rev. Lett. **93**, 267001 (2004).
 - ⁷ D.C. Johnston Phys. Rev. Lett. **62**, 957 (1989).
 - ⁸ T. Nakano, M. Oda, C. Manabe, N. Momono, Y. Miura, and M. Ido, Phys. Rev. B **49**, 16000 (1994).
 - ⁹ H. Takagi, B. Batlogg, H. L. Kao, J. Kwo, R. J. Cava, J. J. Krajewski, and W. F. Peck, Jr., Phys. Rev. Lett. **69**, 2975 (1992).
 - ¹⁰ T. Shibauchi, L. Krusin-Elbaum, M. Li, M.P. Maley, and P. H. Kes, Phys. Rev. Lett. **86**, 5763 (2001); L. Krusin-Elbaum, T. Shibauchi, and C.H. Mielke, Phys. Rev. Lett. **92**, 097005 (2004).
 - ¹¹ For a review, *see*, A. Damascelli, Z. Hussain, and Z.-X. Shen, Rev. Mod. Phys. **75**, 473 (2003).
 - ¹² M. Takigawa, A. P. Reyes, P. C. Hammel, J. D. Thompson, R. H. Heffner, Z. Fisk, and K. C. Ott, Phys. Rev. B **43**, 247 (1991); T. Imai, C. P. Slichter, K. Yoshimura, and K. Kosuge, Phys. Rev. Lett. **70**, 1002 (1993).
 - ¹³ H. F. Fong, B. Keimer, P. W. Anderson, D. Reznik, F. Doğan, I. A. Aksay, Phys. Rev. Lett. **75**, 316 (1995); P. Dai, H. A. Mook, S. M. Hayden, G. Aeppli, T. G. Perring, R. D. Hunt, F. Doğan Science **284**, 1344 (1999); H. F. Fong, P. Bourges, Y. Sidis, L. P. Regnault, A. Ivanov, G. D. Gu, N. Koshizuka, B. Keimer, Nature **398**, 588 (1999); H. He, P. Bourges, Y. Sidis, C. Ulrich and L.P. Regnault, S. Pailhès, N.S. Berzigiarova, N.N. Kolesnikov, B. Keimer, Science **295**, 1045 (2002).
 - ¹⁴ Z. A. Xu, N.P. Ong, Y. Wang, T. Kakheshita, and S. Uchida, Nature (London) **406**, 486 (2000).
 - ¹⁵ Y. Wang, Z. A. Xu, T. Kakheshita, S. Uchida, S. Ono, Y. Ando, and N. Ong, Phys. Rev. B **64**, 224519 (2001).
 - ¹⁶ Y. Wang, Z.A. Xu, Z. A. Xu, T. Kakheshita, S. Uchida, D. A. Bonn, R. Liang, and W. N. Hardy, Phys. Rev. Lett. **88**, 257003 (2002).
 - ¹⁷ Y. Wang, S. Ono, Y. Onose, G. Gu, Y. Ando, Y. Tokura, S. Uchida, and N. Ong, Science **299**, 86 (2003).

- ¹⁸ H. H. Wen, Z. Y. Liu, Z. A. Xu, Z. Y. Weng, F. Zhou, and Z. X. Zhao, Europhys. Lett. **63**, 583 (2003).
- ¹⁹ Yayu Wang, Lu Li, M. J. Naughton, G. D. Gu, S. Uchida, N. P. Ong, Phys. Rev. Lett. **95**, 247002 (2005); L. Li, Y. Wang, M. J. Naughton, S. Ono, Y. Ando, and N. P. Ong, Europhys. Lett. **72**, 451 (2005).
- ²⁰ Y. Wang, L. Li and N. P. Ong, Phys. Rev. B **73**, 024510 (2006).
- ²¹ J. Corson et al. Nature **398**, 221 (1999).
- ²² V.J. Emery and S.A. Kivelson, Nature **374**, 434 (1995).
- ²³ Z. Y. Weng and V. N. Muthukumar, Phys. Rev. B **66**, 094509 (2002).
- ²⁴ O. Vafect and Z. Tesanovic, Phys. Rev. Lett. **91**, 237001 (2003).
- ²⁵ C. Honerkamp and P. A. Lee, Phys. Rev. Lett. **92**, 177002 (2004).
- ²⁶ V. Oganesyan, D.A. Huse, and S. L. Sondhi, to appear in Phys. Rev. B; cond-mat/0502224.
- ²⁷ P. W. Anderson, Phys. Rev. Lett. **96**, 017001 (2006).
- ²⁸ see, Z.Y. Weng, in Proceedings of the International Symposium on Frontiers of Science, 2002 Beijing, (World Scientific 2003); cond-mat/0304261.
- ²⁹ Z. Y. Weng, D. N. Sheng, Y.-C. Chen, and C. S. Ting, Phys. Rev. B **55**, 3894 (1997); D. N. Sheng, Y. C. Chen, and Z. Y. Weng, Phys. Rev. Lett. **77**, 5102 (1996).
- ³⁰ Z.Y. Weng, D. N. Sheng, C. S. Ting, Phys. Rev. Lett. **80**, 5401 (1998); Phys. Rev. B **59**, 8943 (1999).
- ³¹ S.P. Kou and Z.Y. Weng, Phys. Rev. Lett. **90**, 15700 (2003).
- ³² S. P. Kou, X. L. Qi, and Z. Y. Weng, Phys. Rev. B **71**, 235102 (2005).
- ³³ Z. Y. Weng, Y. Zhou, and V. N. Muthukumar, Phys. Rev. B **72**, 0145031 (2005).
- ³⁴ Z.C. Gu and Z.Y. Weng, Phys. Rev. B **72**, 104520 (2005).
- ³⁵ W. Q. Chen and Z. Y. Weng, Phys. Rev. B **71**, 134516 (2005).
- ³⁶ Z. C. Gu, T. Li, and Z. Y. Weng, Phys. Rev. B **71**, 064502 (2005).
- ³⁷ V. N. Muthukumar and Z. Y. Weng, Phys. Rev. B **65**, 174511 (2002).
- ³⁸ M. Shaw, Z. Y. Weng, and C. S. Ting, Phys. Rev. B **68**, 014511 (2003).
- ³⁹ P. W. Anderson, J. Phys. Chem. Solids, **63**, 2145 (2002), cond-mat/0108522; *ibid.*, Physica B **318**, 28 (2002), cond-mat/0201431.
- ⁴⁰ P. W. Anderson, Science **235**, 1196 (1987); G. Baskaran, Z. Zou, and P. W. Anderson, Solid State Commun. **63**, 973 (1987); G. Kotliar and J. Liu, Phys. Rev. B **38**, 5142 (1988); P. W. Anderson, P. A. Lee, M. Randeria, T. M. Rice, N. Trivedi, and F. C. Zhang, J. Phys.: Condens. Matter **16**, R755 (2004).
- ⁴¹ Z. Y. Weng, D. N. Sheng, and C. S. Ting, Phys. Rev. B **61**, 12328 (2000); Y. Zhou, V. N. Muthukumar, and Z. Y. Weng, Phys. Rev. B **67**, 064512 (2003).
- ⁴² L. B. Ioffe and A. I. Larkin, Phys. Rev. B **39**, 8988 (1989).
- ⁴³ N. Nagaosa and P. A. Lee, Phys. Rev. Lett. **64**, 2450 (1990); P. A. Lee and N. Nagaosa, Phys. Rev. B **46**, 5621 (1992).
- ⁴⁴ X.-G. Wen and P.A. Lee, Phys. Rev. Lett. **76**, 503 (1996); P. A. Lee, N. Nagaosa, T.-K. Ng, X.-G. Wen, Phys. Rev. B **57**, 6003 (1998).
- ⁴⁵ T. Senthil and Matthew P.A. Fisher, Phys. Rev. B **62**, 7850 (2000); Phys. Rev. B **63**, 134521 (2001).
- ⁴⁶ One may also directly use the GL equation (15) to get a similar approximate estimate for T_v , by rewriting it in the form $(-i\nabla - \mathbf{A}^s)^2\psi_h = (1/\xi_h^2)(1 - |\psi_h|^2/\rho_h^0)\psi_h$ and by noting that $\xi_h \equiv 1/\sqrt{2m_h(-\alpha)} >$ the average holon-holon inter-distance $\sim a_c$ while $(-i\nabla - \mathbf{A}^s)^2\psi_h \sim (1/a_c^2)\psi_h$ in the vortex packing limit.
- ⁴⁷ H. H. Wen, H. Gao, Z. Y. Liu, F. Zhou, J. Xiong, W. Ti, to be published;
- ⁴⁸ S.P. Kou, X.L. Qi, and Z.Y. Weng, Phys. Rev. B **72**, 165114 (2005).
- ⁴⁹ X. L. Qi and Z. Y. Weng, unpublished.
- ⁵⁰ see, P. Bourges, in *The Gap Symmetry and Fluctuations in High Temperature Superconductors*, Ed. by J. Bok *et al* (Plenum Press, 1998).